Ultrafast Imaging of Plasmonic Vortex Fields with Axion-type Response

Atreyie Ghosh, Sena Yang, Yanan Dai, Amit Bhoonah, Vincent Liu, Brian Batell and Hrvoje Petek.
IQ Initiative, Department of Physics and Astronomy, University of Pittsburgh.

April 7, 2023
Axions, Fundamental and Synthetic Workshop

Background Story & Motivation

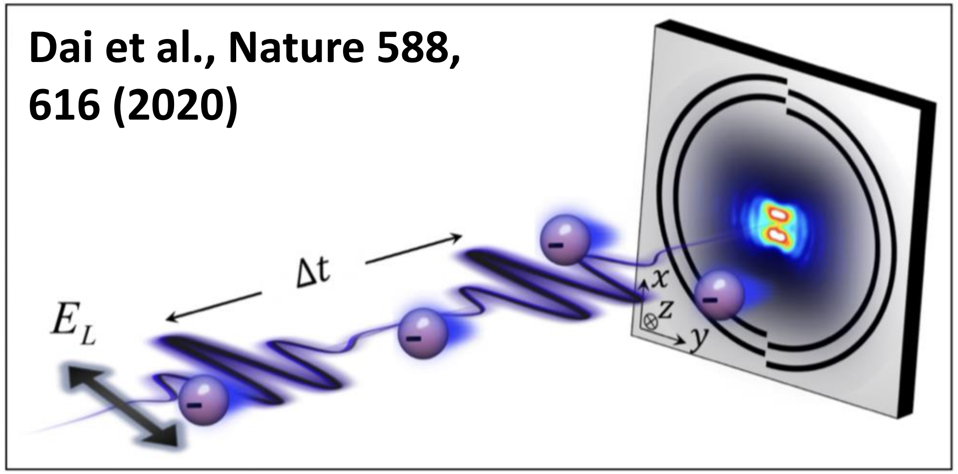

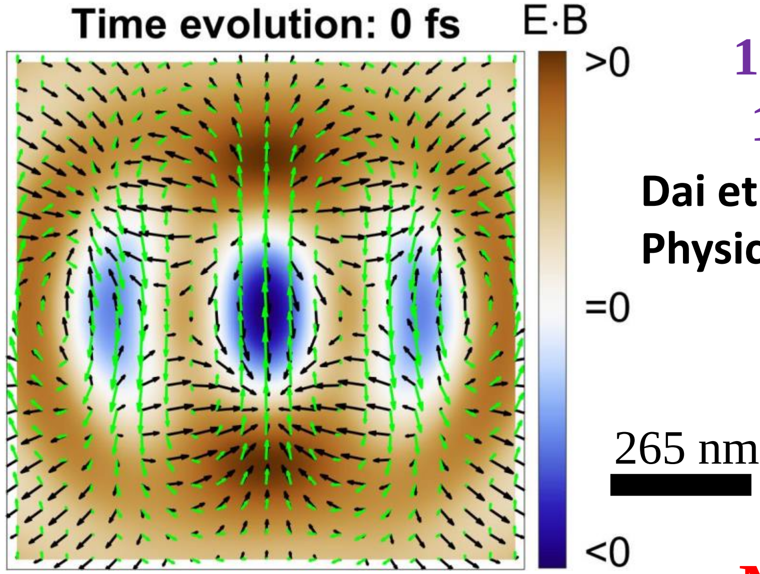

$1\ \text{nm} = 10^{-9}\ \text{m}$

$1\ \text{fs} = 10^{-15}\ \text{s}$

Dai et al., Nature Reviews Physics 4, 562-564 (2022)

PRL **113,** 033601 (2014) PHYSICAL REVIEW LETTERS

Magnetoelectric Effects in Local Light-Matter Interactions

Konstantin Y. Bliokh,[1,2] Yuri S. Kivshar,[3] and Franco Nori[2,4]
[1]*iTHES Research Group, RIKEN, Wako-shi, Saitama 351-0198, Japan*
[2]*CEMS, RIKEN, Wako-shi, Saitama 351-0198, Japan*
[3]*Nonlinear Physics Center, Research School of Physics and Engineering, Australian National University, Canberra ACT 0200, Australia*
[4]*Physics Department, University of Michigan, Ann Arbor, Michigan 48109-1040, USA*

(Received 30 December 2013; published 16 July 2014)

We study the generic dipole interaction of a monochromatic free-space electromagnetic field with a bi-isotropic nanoparticle or a molecule. Contributions associated with the breaking of dual, *P*, and *T* symmetries are responsible for electric-magnetic asymmetry, chirality, and the nonreciprocal magnetoelectric effect, respectively. We calculate absorption rates, radiation forces, and radiation torques for the nanoparticle and introduce novel field characteristics quantifying the transfer of energy, momentum, and angular momentum due to the three symmetry-breaking effects. In particular, we put forward a concept of "magnetoelectric energy density," quantifying the local *PT* symmetry of the field. Akin to the "superchiral" light suggested recently for local probing of molecular chirality, here we suggest employing complex fields for a sensitive probing of the nonreciprocal magnetoelectric effect in nanoparticles or molecules.

Magnetoelectric response, $A_{ME} = \dfrac{2\text{Real}(\boldsymbol{E}^* \cdot \boldsymbol{H})}{|\boldsymbol{E}|^2 + \delta|\boldsymbol{H}|^2}$

$$\boldsymbol{E} \propto (\hat{\boldsymbol{x}} + i\sigma\hat{\boldsymbol{y}})e^{ikz} + (\hat{\boldsymbol{x}} + i\sigma\hat{\boldsymbol{y}})e^{-ikz}$$
$$\boldsymbol{H} \propto (\hat{\boldsymbol{y}} - i\sigma\hat{\boldsymbol{x}})e^{ikz} - (\hat{\boldsymbol{y}} - i\sigma\hat{\boldsymbol{x}})e^{-ikz}$$

Magnetoelectric Response at Plasmonic Vortex Core???

Magnetoelectric Response at Plasmonic Vortex Core

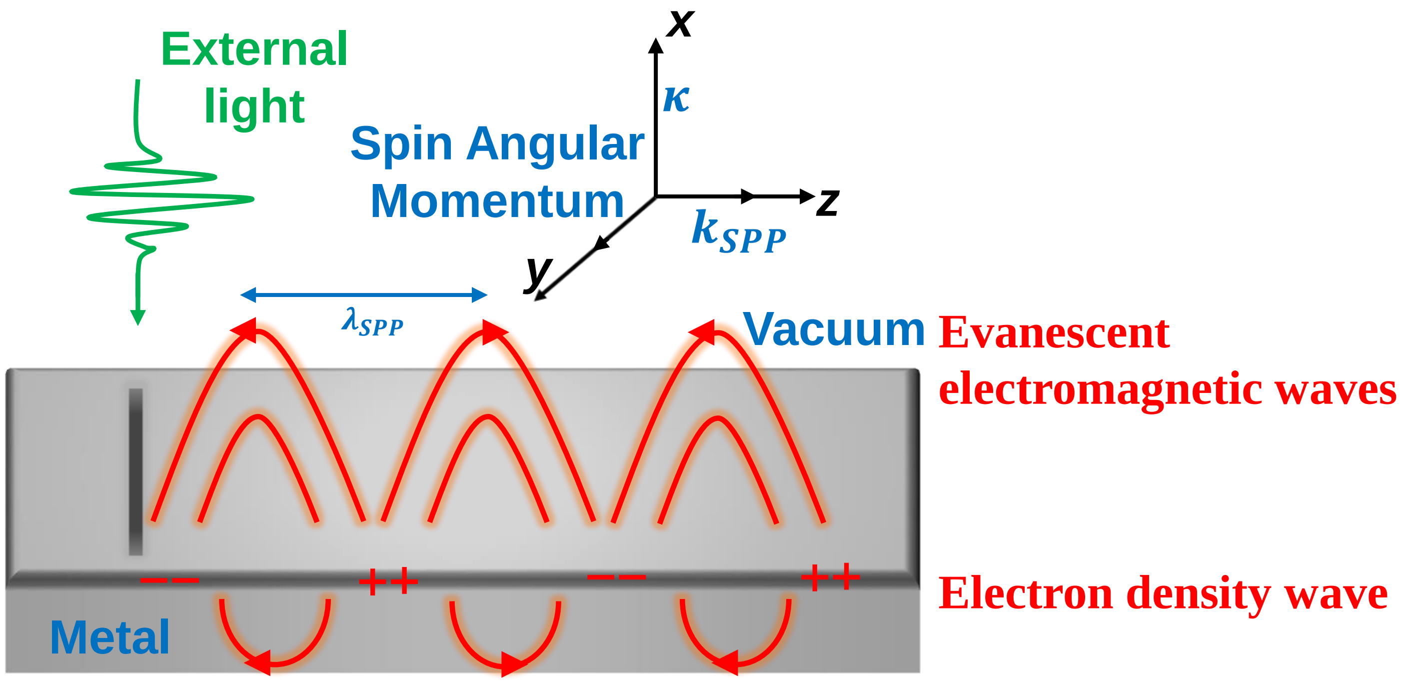

SPP dispersion relation,

$$k_{SPP} = k_0 \sqrt{\frac{\varepsilon_1 \varepsilon_2}{\varepsilon_1 + \varepsilon_2}}$$

Collective oscillations of free electron density generated by light-matter interaction.

Surface plasmon polaritons (SPPs):

Collective charge density fluctuations that can be excited by external optical fields at metal-vacuum interface.

How Do We Generate and Image Plasmonic Vortices?

Interferometric Time Resolved Photoemission Electron Microscopy (ITR-PEEM)

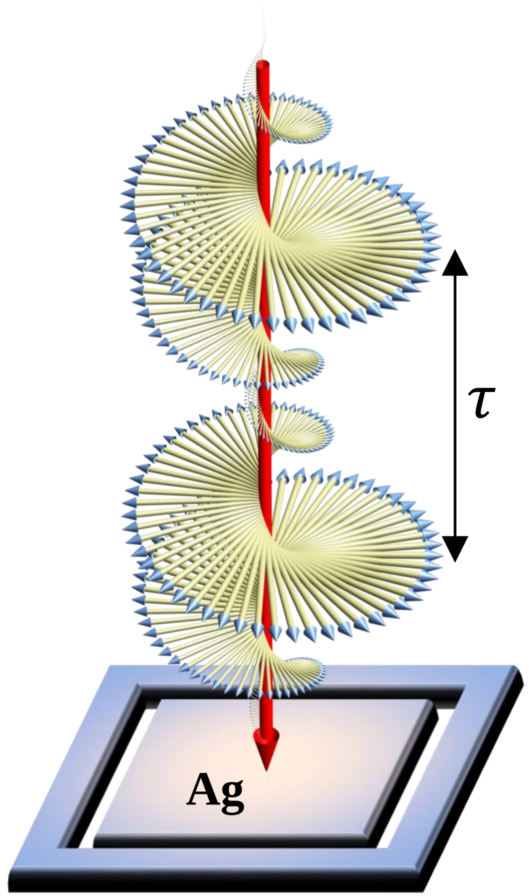

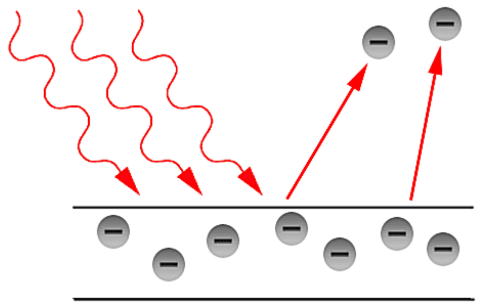

$$\mathrm{E} = h\nu - \phi$$

Photoelectric effect, *Source: Wikipedia*

- Non-linear, two or more photon photoemission (mPP) process.
- PEEM imaging signal,
$$I_{PEEM} \sim \int_{-\infty}^{t} (P_{total}(x, y, \tau'))^{2n} d\tau' .$$
- λ_L=550 nm (2.25 eV), for Ag, n=2, 2PP process.

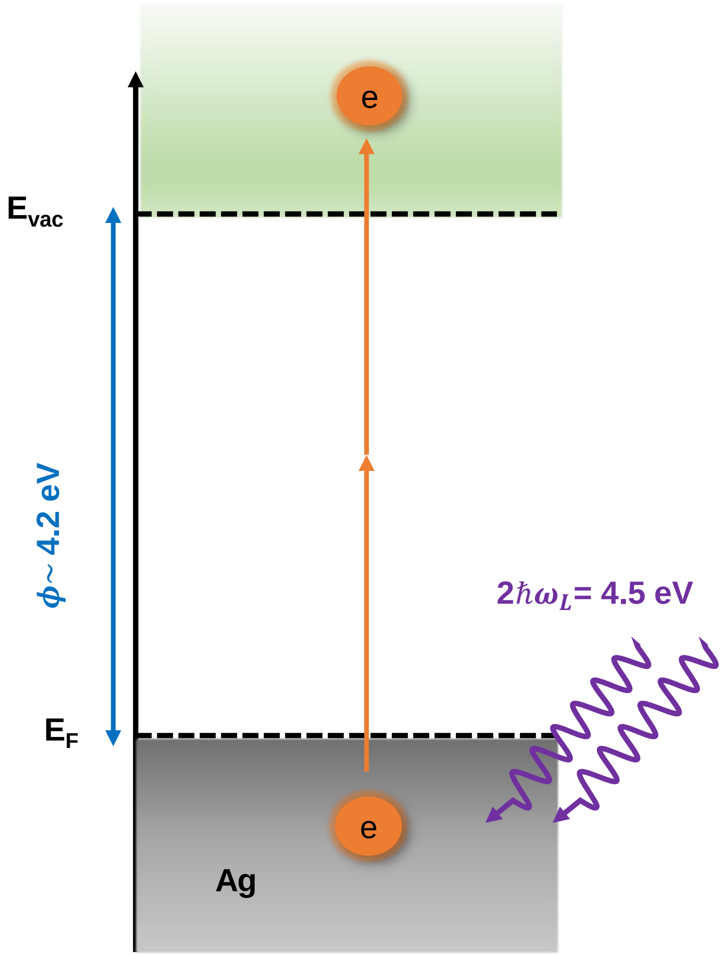

Experimental method: Interferometric time-resolved photoemission electron microscopy (ITR-PEEM)

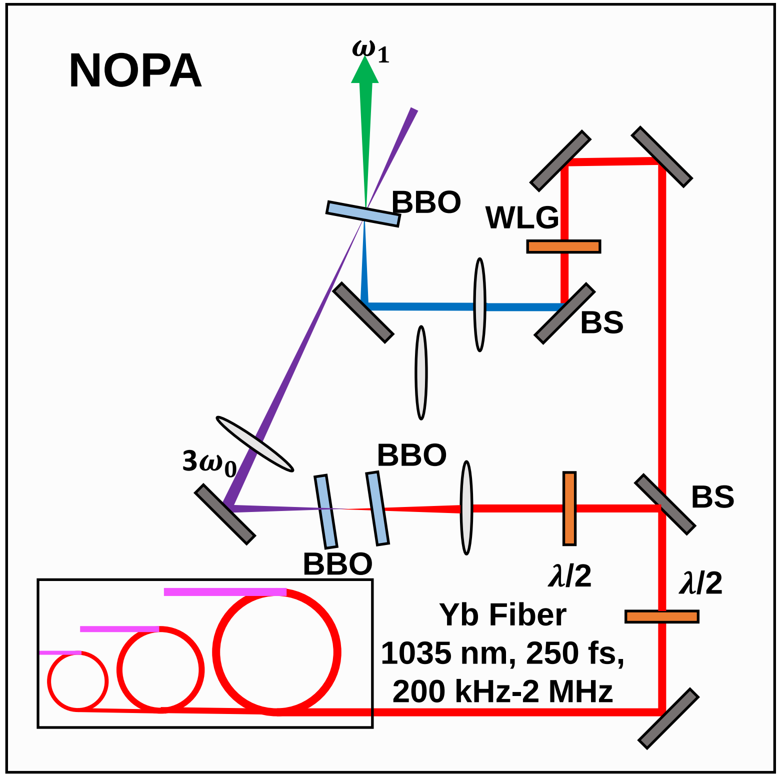

Schematic of NOPA process

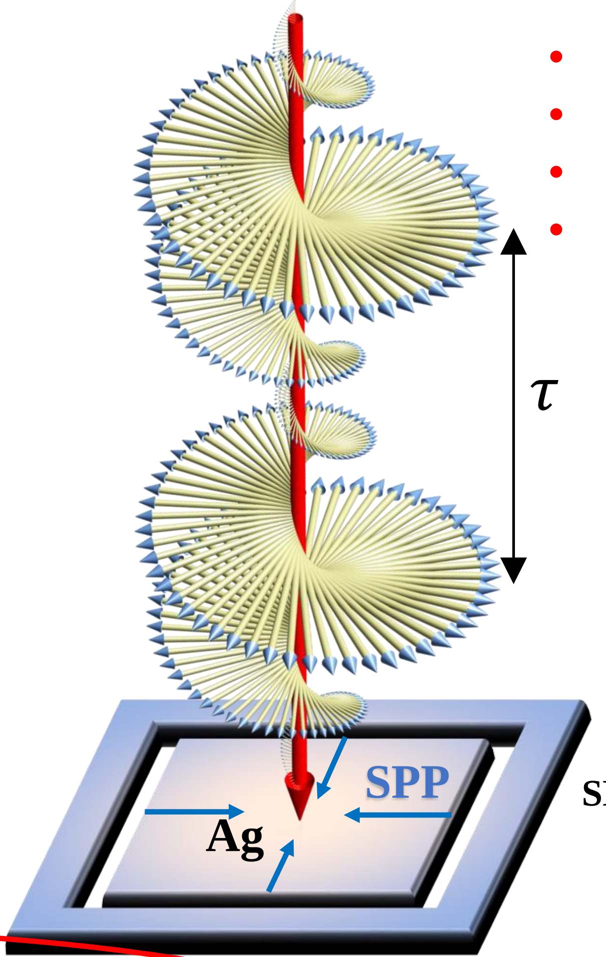

- Normally incident
- Left Circularly polarized ($\sigma = -1$)
- Pulse duration <20 fs
- λ_L=550 nm center wavelength.

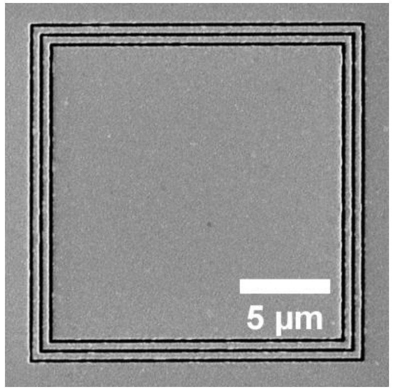

SEM image of nanofabricated sample

λ_{SPP}=530 nm

Among noble metals, Ag holds a unique place because its interband absorption starts only in UV range giving a low loss in visible spectrum.

- 100 nm Ag film on n-type Si(111) substrate
- A square shaped coupling structure
- Focused ion beam (FIB) lithography
- Dimension $30\lambda_{SPP}$

Femtosecond time resolved imaging of Plasmonic Vortices

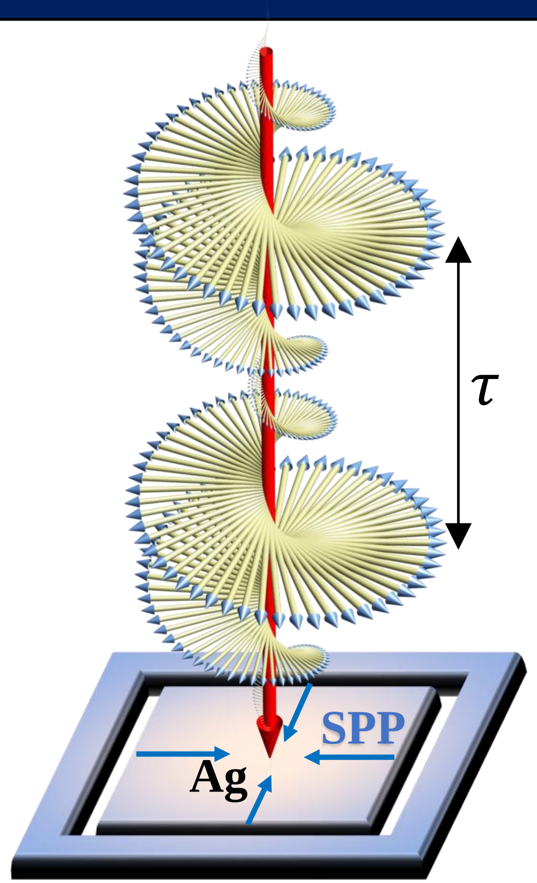

A pair of identical pump-probe pulses with pulse delay τ

Interference of SPP generated by the pump and the optical field of delayed probe

Pixel wise Fourier processing of the raw ITR-PEEM data

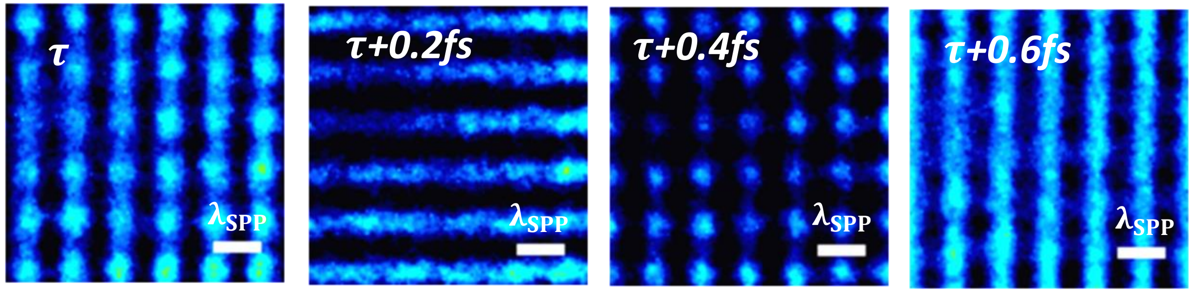

Extracted images

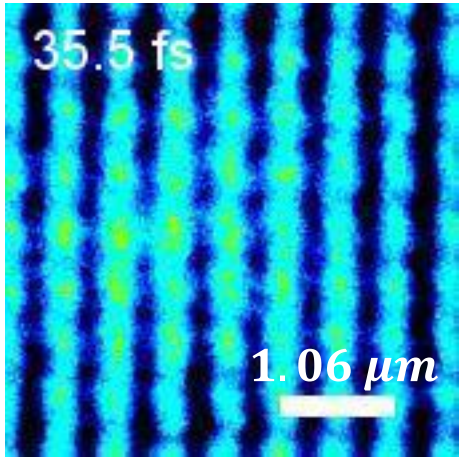

Raw ITR-PEEM data

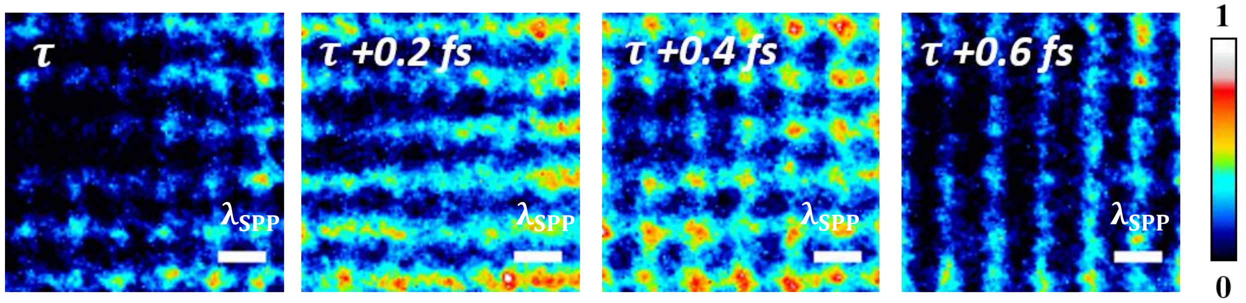

Ghosh et al., Applied Physics Reviews 8, 041413 (2021)

Analytical Model

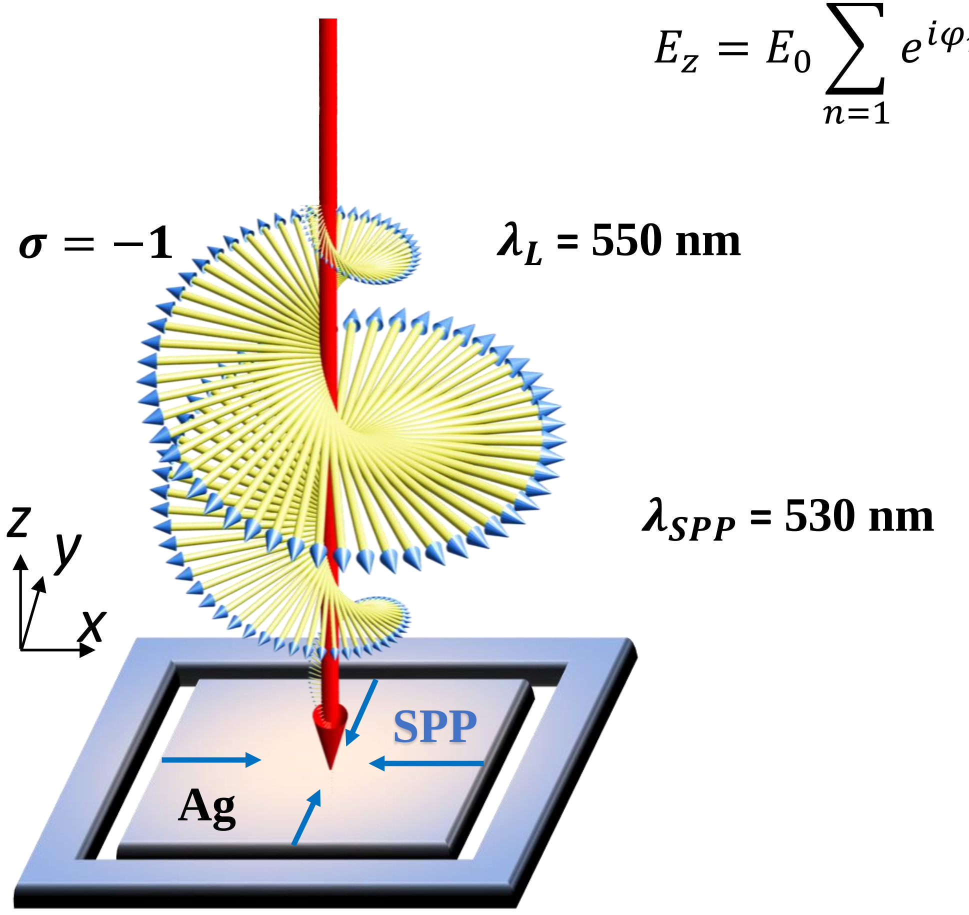

Ghosh et al., ACS Photonics 10, 13-23 (2023)

$$E_z = E_0 \sum_{n=1}^{Q} e^{i\varphi_n} e^{-ik_{SPP}[\sin(\theta_n)x+\cos(\theta_n)y]}$$

k_{SPP}, SPP wave vector

$\theta_n = -\frac{2\pi n}{Q}$, relative angle of k_{SPP} to the y axis

$\varphi_n = \frac{2\pi n\sigma}{Q}$, relative phase of the n^{th} SPP wave

Maxwell's Equations →

$$E_x = E_0 \sum_{n=1}^{Q} i\sin(\theta_n)\, e^{i\varphi_n} e^{-ik_{SPP}[\sin(\theta_n)x+\cos(\theta_n)y]}$$

$$E_y = E_0 \sum_{n=1}^{Q} i\cos(\theta_n)\, e^{i\varphi_n} e^{-ik_{SPP}[\sin(\theta_n)x+\cos(\theta_n)y]}$$

$$H_x = E_0 \sum_{n=1}^{Q} k_{SPP}\cos(\theta_n)\, e^{i\varphi_n} e^{-ik_{SPP}[\sin(\theta_n)x+\cos(\theta_n)y]}$$

$$H_y = E_0 \sum_{n=1}^{Q} -k_{SPP}\sin(\theta_n)\, e^{i\varphi_n} e^{-ik_{SPP}[\sin(\theta_n)x+\cos(\theta_n)y]}$$

$$H_z = 0$$

(Anti) Parallel *E* and *H* fields at Plasmonic Vortex Cores

SPP phase: colormap showing phase of the out-of-plane SPP electric field (E_z), along with SPP Poynting vector (k_{SPP}) distribution (arrows),

Colormap: $Re(\boldsymbol{E}^* \cdot \boldsymbol{H})$,
Black arrows: ***E*** fields
Green Arrows: ***H*** fields

$Re(E^* \cdot H)$ is constant over the pulse duration (~20 fs in this case)!

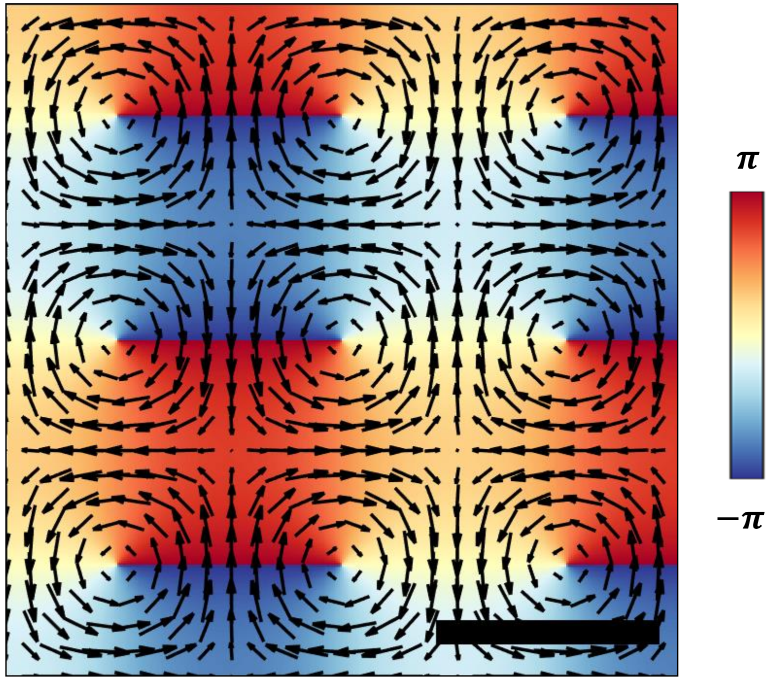

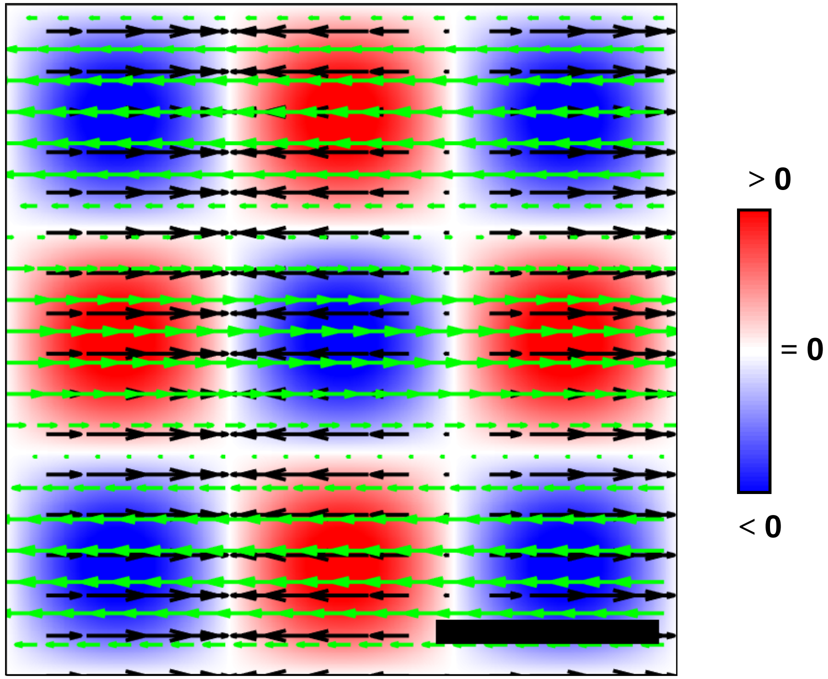

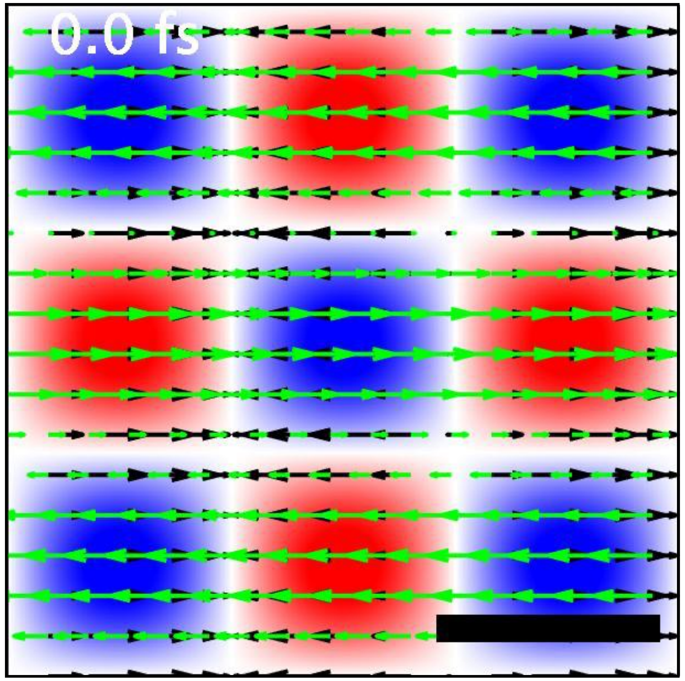

Scale bars represent, $\frac{\lambda_{SPP}}{2} = 265$ nm

Ability to study $(E^* \cdot H)$ in subwavelength spatial and suboptical cycle time scale

Quantification of Magnetoelectric Response from Plasmonic Vortices

SPP phase: colormap showing phase of the out-of-plane SPP electric field (E_z), along with SPP Poynting vector (k_{SPP}) distribution (arrows),

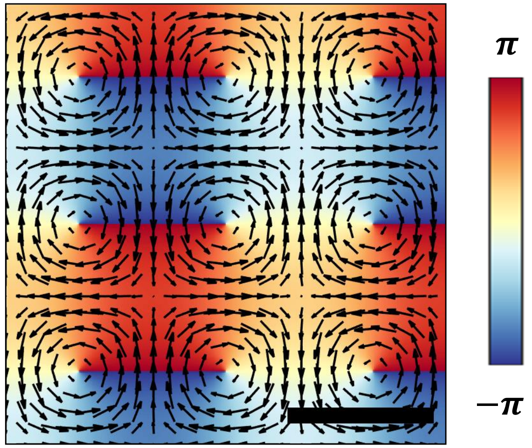

Colormap: $Re(\boldsymbol{E}^* \cdot \boldsymbol{H})$,
Black arrows: $\boldsymbol{E}$ fields
Green Arrows: $\boldsymbol{H}$ fields

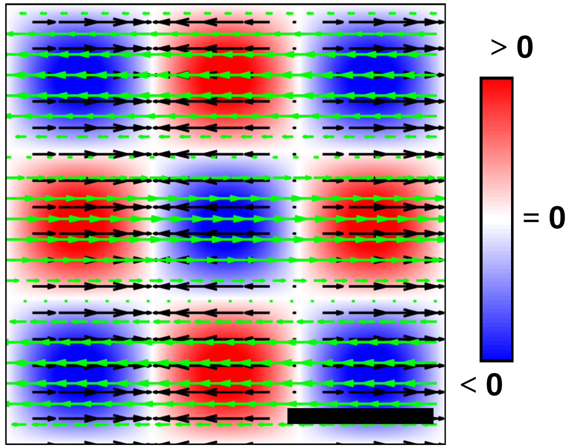

$$A_{ME} = \frac{2\text{Real}(\boldsymbol{E}^* \cdot \boldsymbol{H})}{|\boldsymbol{E}|^2 + \delta|\boldsymbol{H}|^2}$$

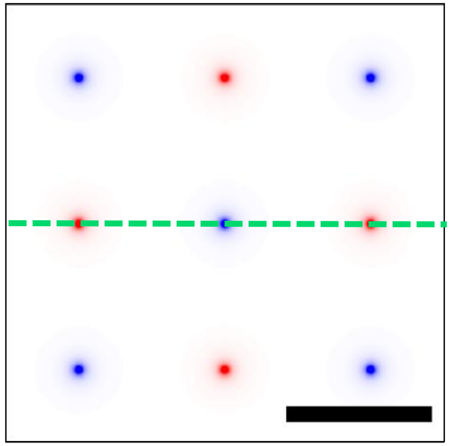

Height: 12.5
Full Width Half Maxima: 10.34 nm

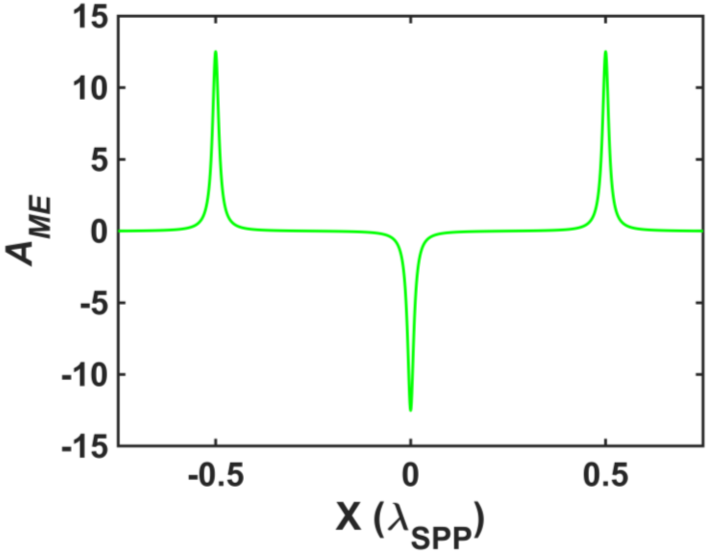

Scale bars represent, $\frac{\lambda_{SPP}}{2} = 265$ nm

Scale bars represent, $\frac{\lambda_{SPP}}{2} = 265$ nm

SPP phase: colormap showing phase of the out-of-plane SPP electric field (E_z), along with SPP Poynting vector (k_{SPP}) distribution (arrows),

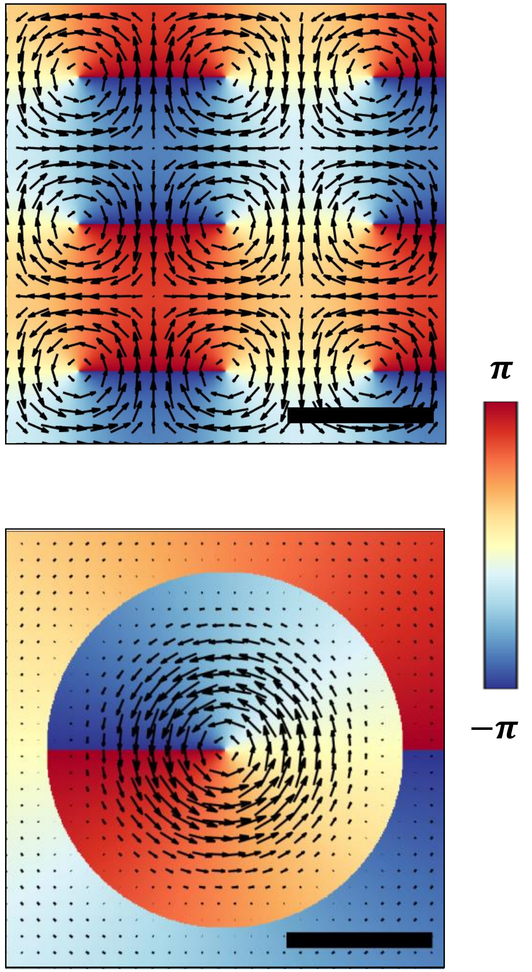

Colormap: $Re(\boldsymbol{E}^* \cdot \boldsymbol{H})$,
Black arrows: $\boldsymbol{E}$ fields
Green Arrows: $\boldsymbol{H}$ fields

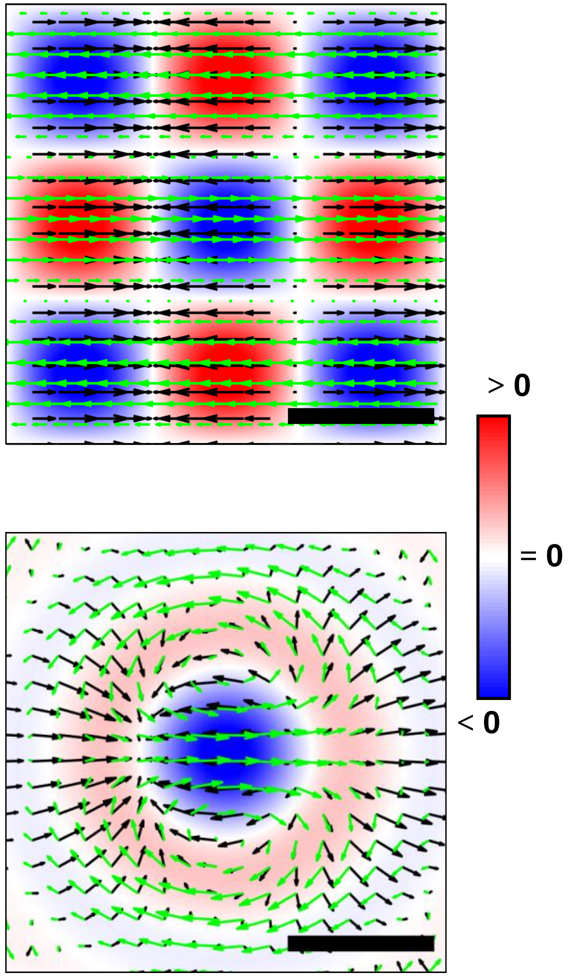

$$A_{ME} = \frac{2\mathrm{Real}(\boldsymbol{E}^* \cdot \boldsymbol{H})}{|\boldsymbol{E}|^2 + \delta|\boldsymbol{H}|^2}$$

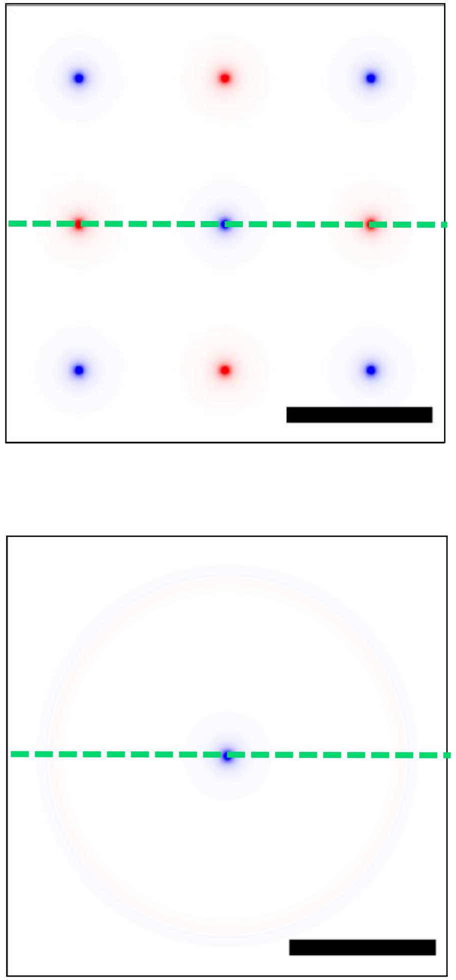

Height: 12.5
Full Width Half Maxima: 10.34 nm

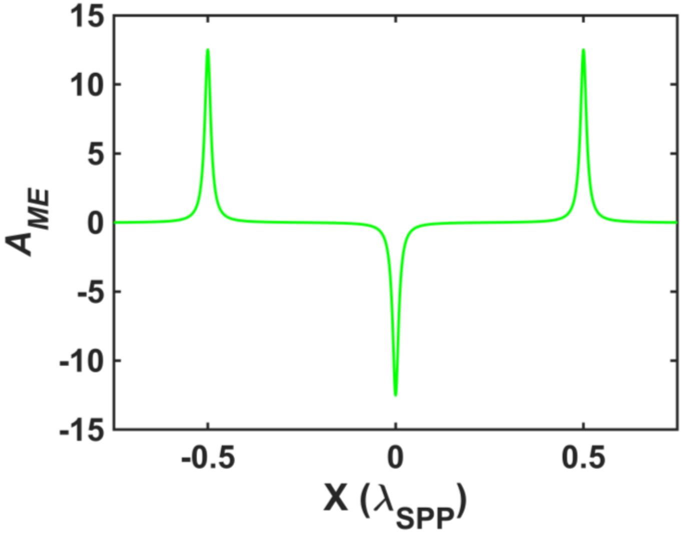

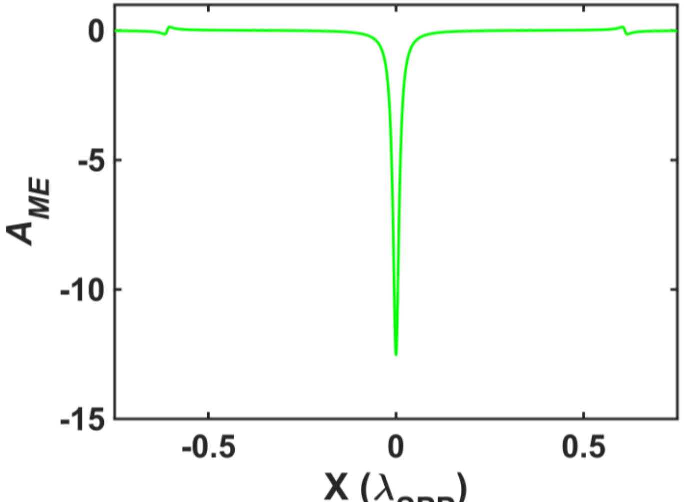

$$A_{ME} = \frac{2\mathrm{Real}(\boldsymbol{E}^{*} \cdot \boldsymbol{H})}{|\boldsymbol{E}|^2 + \delta|\boldsymbol{H}|^2}$$

Hexagonal Symmetry

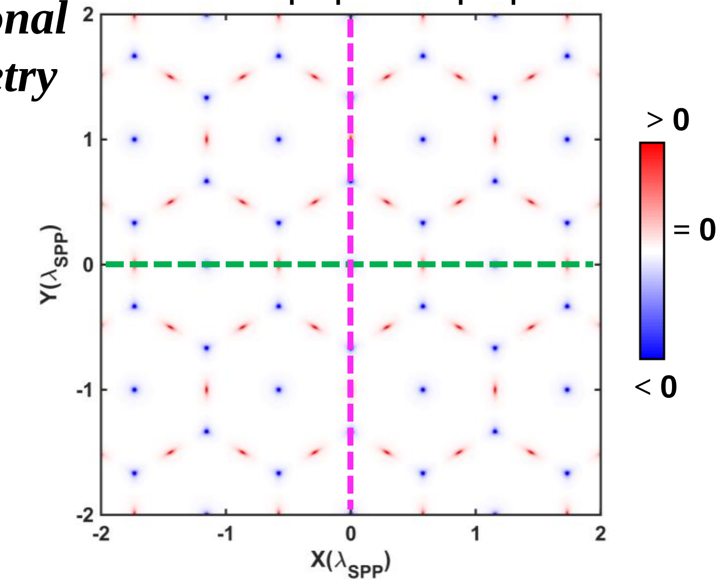

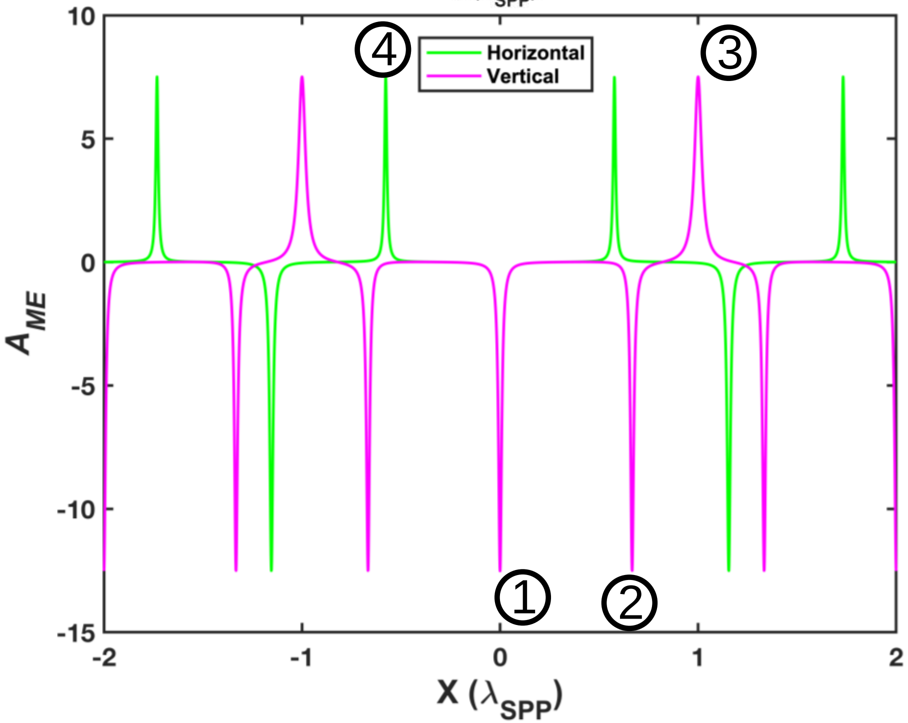

① **FWHM = 10.34 nm**

② **FWHM = 10.07 nm**

③ **FWHM = 22.53 nm**

④ **FWHM = 7.42 nm**

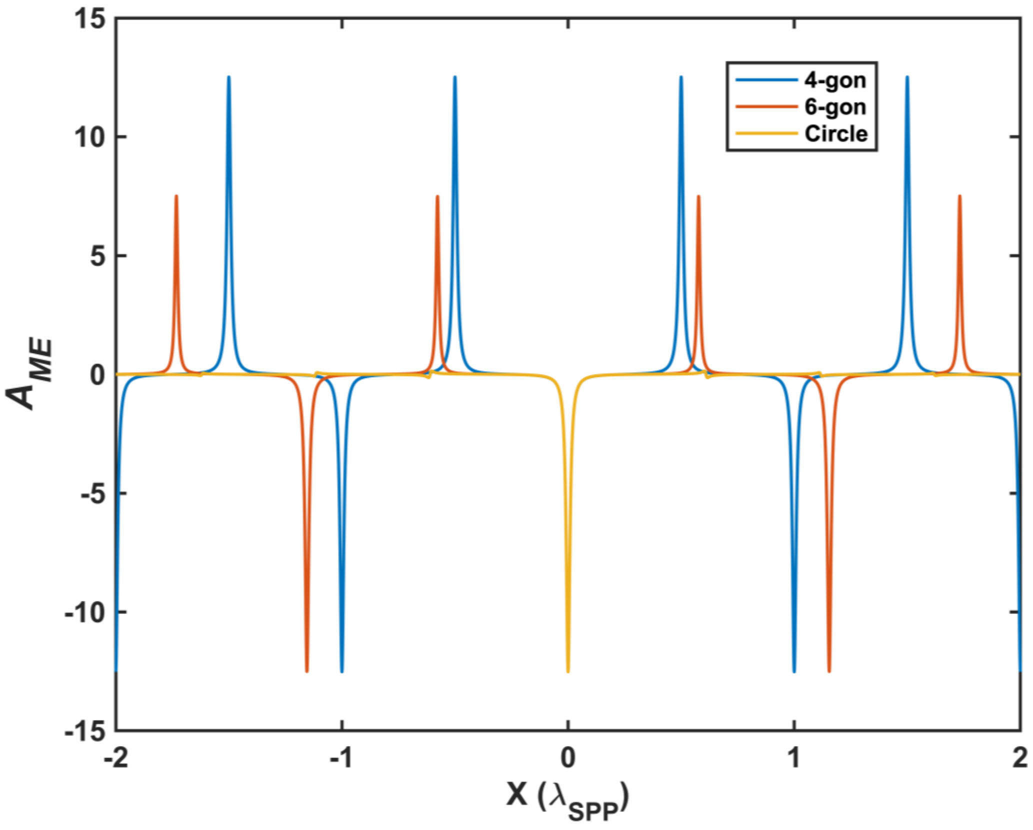

Verification from ITR-PEEM Data

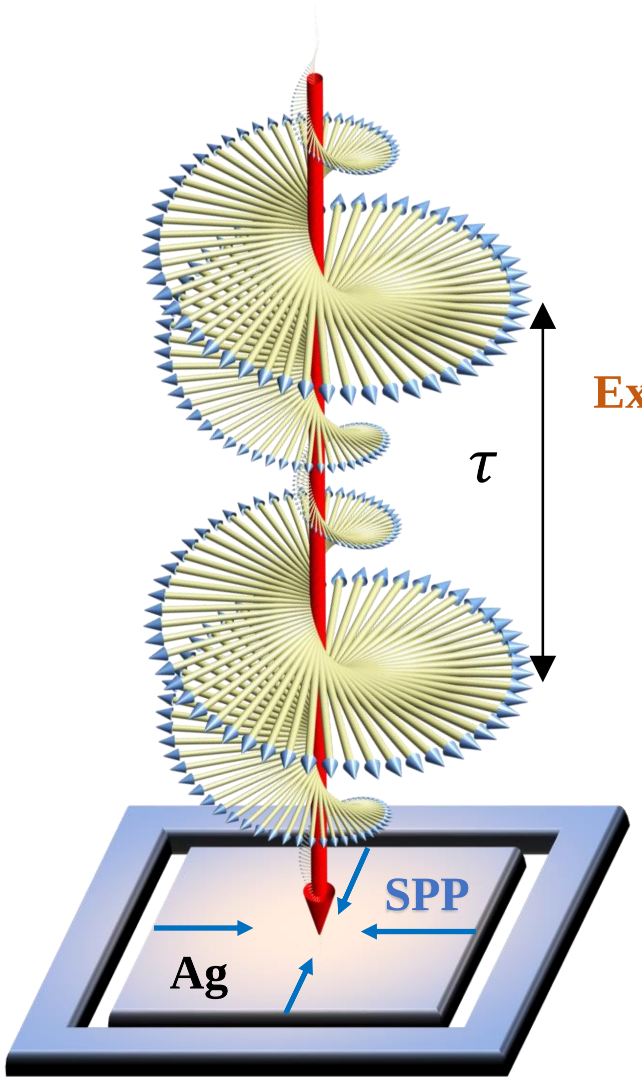

Extracting SPP *E* and *H* field components

Excellent Match !

Colormap: $Re(\boldsymbol{E}^* \cdot \boldsymbol{H})$,
Black arrows: ***E*** fields
Green Arrows: ***H*** fields

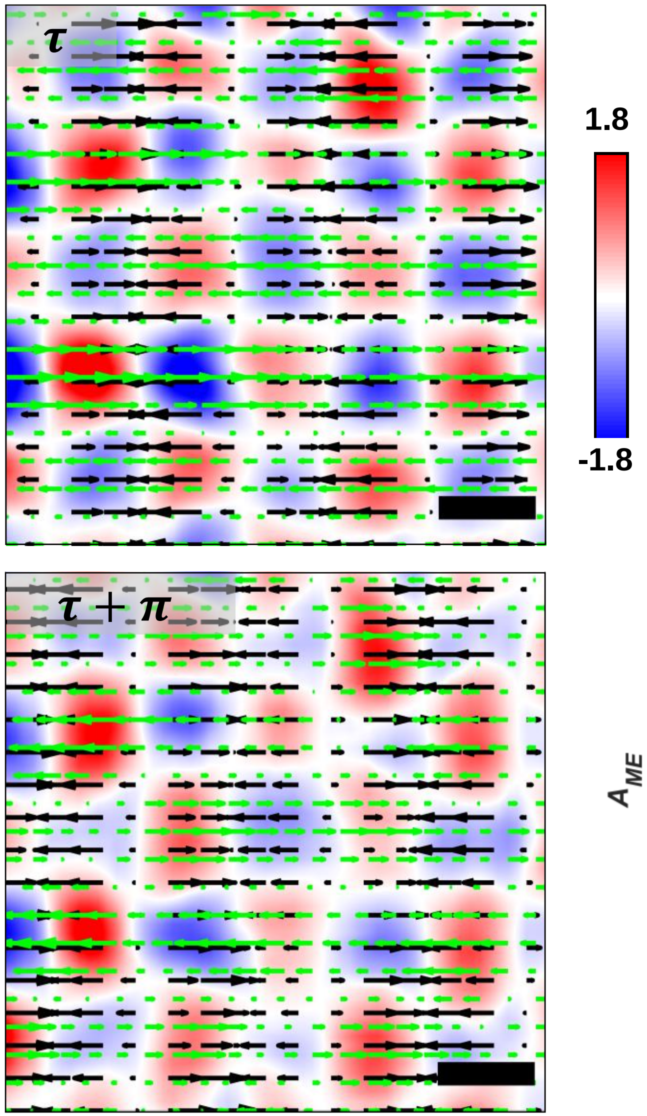

$$A_{ME} = \frac{2\mathrm{Real}(\boldsymbol{E}^* \cdot \boldsymbol{H})}{|\boldsymbol{E}|^2 + \delta|\boldsymbol{H}|^2}$$

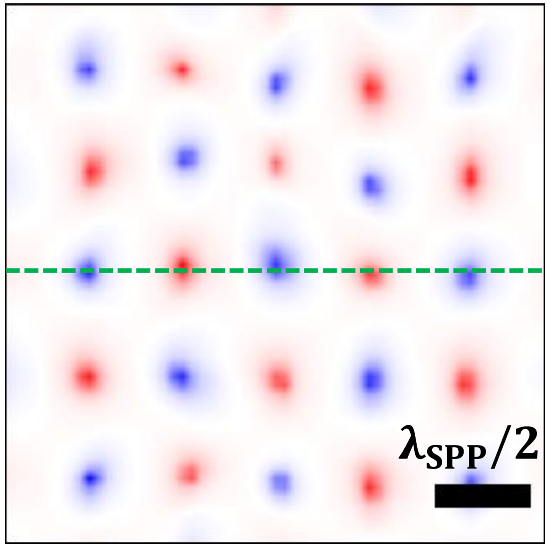

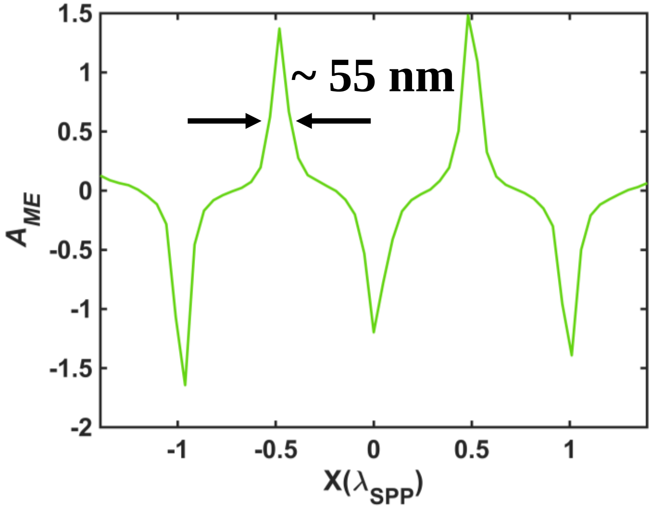

Scale bars represent, $\frac{\lambda_{SPP}}{2} = 265$ nm

Axion Response at Plasmonic Vortex Cores

Plasmonic vortex cores are strong, localized, and stable sources of $(\boldsymbol{E}^* \cdot \boldsymbol{H})$ response

↓

Suitable platform for $\boldsymbol{E}^* \cdot \boldsymbol{H}$ quasiparticle excitations for dressing axion electrodynamics

↓

Investigation of Axion Response from Plasmonic Vortex Cores

GOAL: Axion Production Rate from Plasmonic Vortices

IQ Initiative

Axion Production Rate: General Set-up

- Axion Equations of Motion,

$$\partial_t^2 a - \nabla^2 a + m_a^2 a = g_{a\gamma\gamma} \boldsymbol{E}^* \cdot \boldsymbol{H}$$

- At classical level, this is a wave equation with a source $g_{a\gamma\gamma} \boldsymbol{E}^* \cdot \boldsymbol{H}$.

- When number of axion particle created is large, classical behavior is valid.

- When the number of axion particle created is small, a semi-classical approximation used: particle creation by a classical source.

- Mean number of particles created by a plasmonic vortex given by,

$$N_{ax} = \int \frac{d^3k}{(2\pi)^3} \frac{1}{2\omega_k} |\mathcal{F}(\boldsymbol{E}^* \cdot \boldsymbol{H})|^2$$

with $\omega_k^2 = |\boldsymbol{k}|^2 + m_a^2$

Source Modeling

Spatial Variation: Fourier Transformation Done Numerically

Time Variation: $\boldsymbol{E}^* \cdot \boldsymbol{H}$ non-zero on femto-second time scale

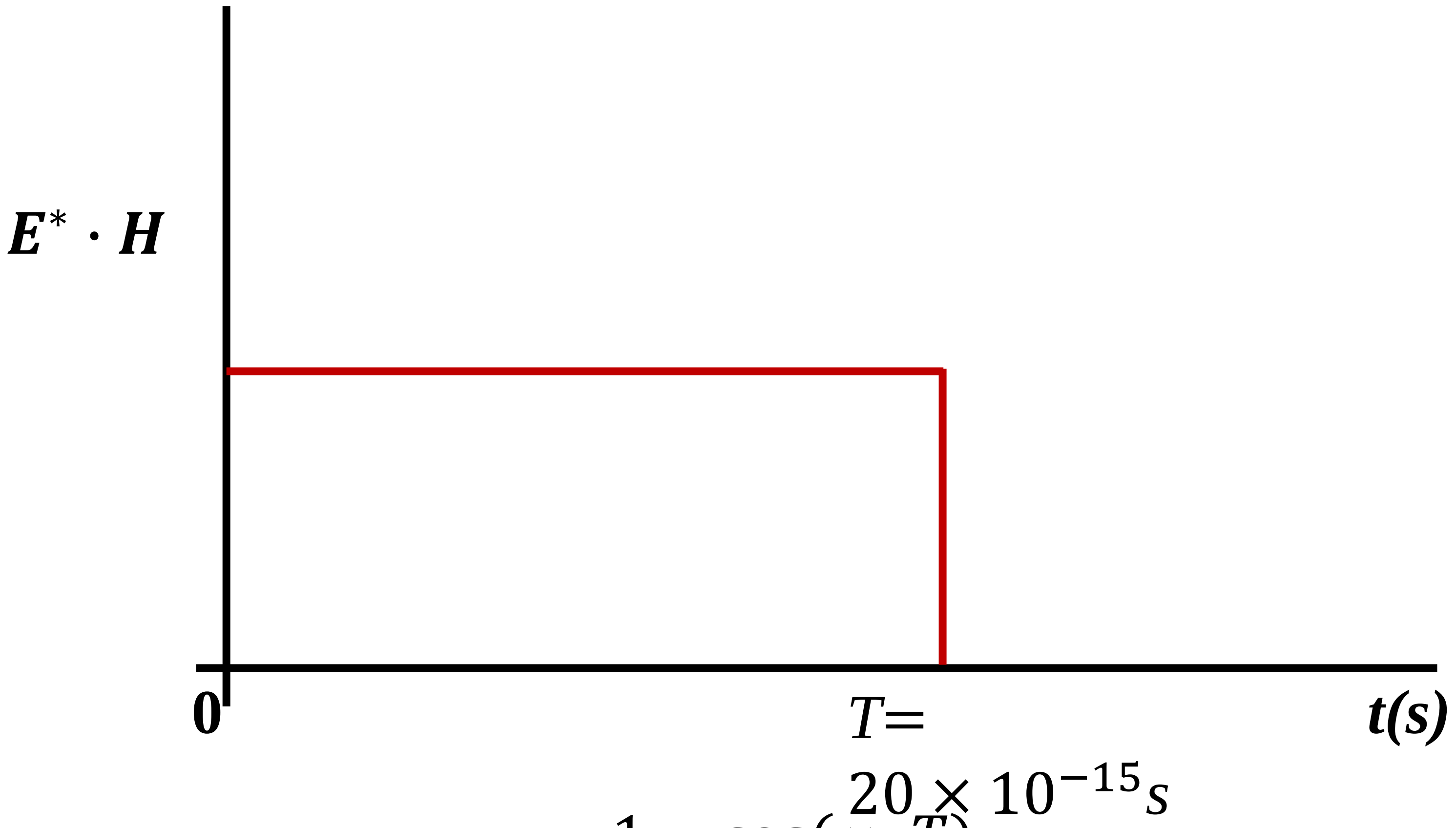

$$|\mathcal{F}(\boldsymbol{E}^* \cdot \boldsymbol{H})|^2 \propto 2\frac{1-\cos(\omega_k T)}{\omega_k^2}|\boldsymbol{j}(\boldsymbol{k})|^2$$

Axion Production Rate: From a single Plasmonic Vortex

Begin with the simplest possible case:
Isolated Single Circular Vortex

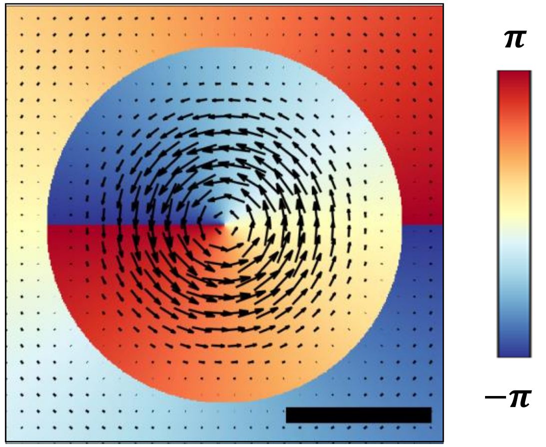

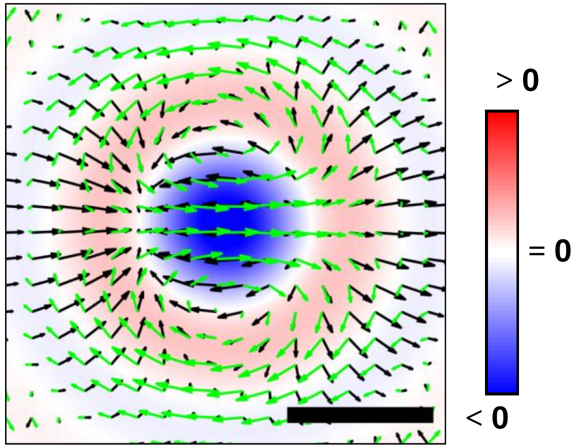

$$E_z(r,\theta,z=0) = -E_0 \frac{2i\pi R k_{SPP}}{\omega_{SPP}\varepsilon_0\varepsilon_d} e^{ik_{SPP}} e^{i\theta} J_1(k_{SPP} r)$$

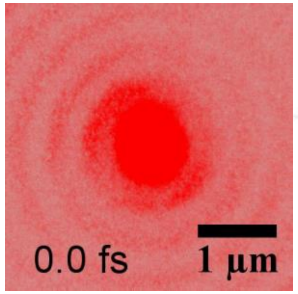

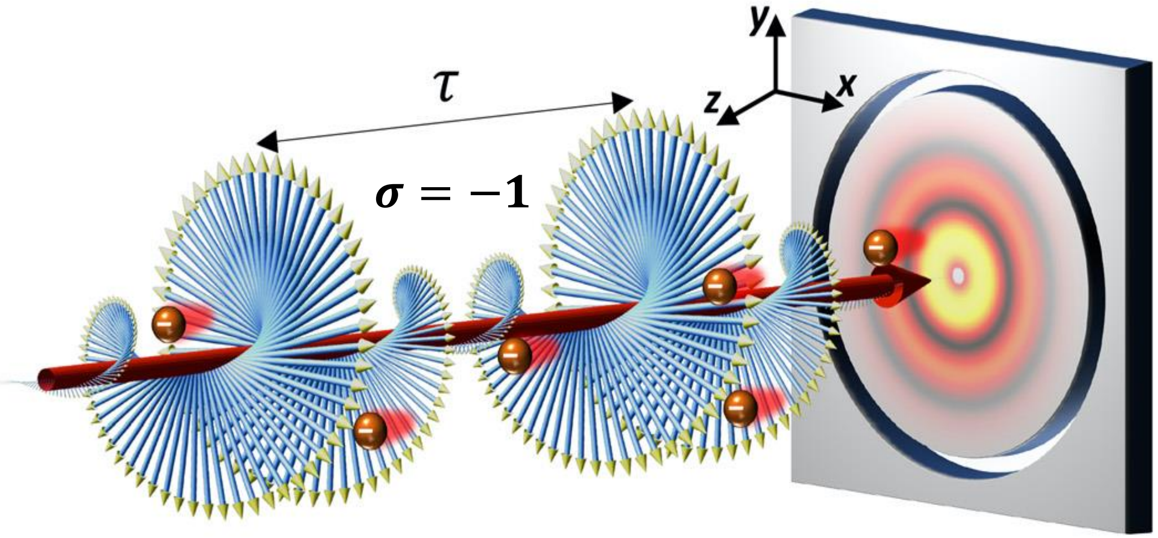

Deduce $(E^* \cdot H)$ and N_{ax}

Ongoing Work!

Dai et al., Applied Physics Reviews 9, 011420 (2022)

Axion Production Rate: From a single Plasmonic Vortex

Parametrically, Axion Production Rate scales as $\sim g_{a\gamma\gamma}^2 (\frac{E_0 H_0 \pi R^2 \kappa \pi}{\varepsilon_0 \varepsilon_d \omega_{SPP}})^2 \frac{1-\cos(\omega_k T)}{\omega_k^2} |\boldsymbol{j}(\boldsymbol{k})|^2$

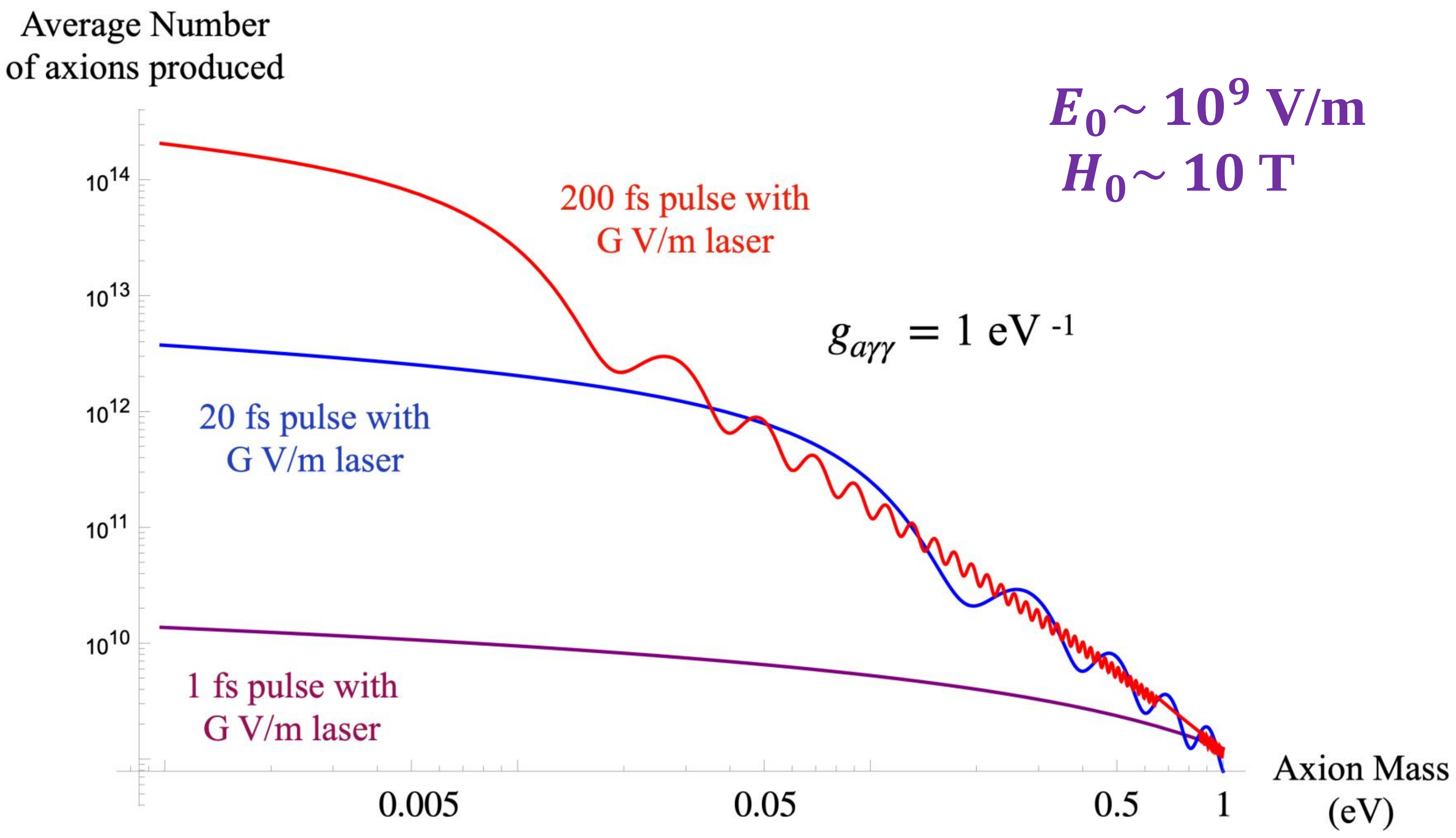

$E_0 \sim 10^9$ V/m
$H_0 \sim 10$ T

- **Without need of external source!**
- **Simple setup**

Summary & Future Scopes

We provide robust analysis of plasmonic supermagnetoelectric fields in a single vortex and vortex arrays launched within polygonal coupling structures that exhibit $E||H$ field. The vortex cores appear as strong and stable source of $(E^* \cdot H)$ response confined in subwavelength ($<\lambda_{SPP}/2$) scale.

We experimentally verify the existence of strong, stable and localized $(E^* \cdot H)$ response from plasmonic vortex cores in the visible regime by ultrafast microscopy imaging and achieved a focus of $(E^* \cdot H)$ on the length scale of $\lambda_{SPP}/10$.

The ability to generate, design and image interactions of $(E^* \cdot H)$ fields on nanometer (10^{-9} m) spatial and femtosecond (10^{-15} s) temporal scales provides an excellent opportunity to explore Axion physics beyond the Standard Model.

Immediate goal is to introduce a complete and accurate theoretical picture of axion production from plasmonic vortices by setting up the associated parameters with utmost precision.

Long term goal is to develop experimental methodology that can det
from plasmonic vortices with "synthetic" axion matter. One candida

Narang et al., Nature Reviews Physics, 2, 682-696 (2020)

Acknowledgements

Laboratory of ultrafast dynamics

Prof. Hrvoje Petek
Prof. Vincent Liu
Prof. Brian Batell
(University of Pittsburgh)

Prof. Yanan Dai,
(Southern University of Science and Technology, China)

Dr. Sena Yang
Dr. Amit Bhoonah

THANK YOU!!!

PITTSBURGH QUANTUM INSTITUTE
www.pqi.org

UNIVERSITY OF PITTSBURGH
VERITAS 1787 VIRTUS